Science Advances
AAAS

advances.sciencemag.org/cgi/content/full/5/6/eaav4275/DC1

Supplementary Materials for

Epithelial-type systemic breast carcinoma cells with a restricted mesenchymal transition are a major source of metastasis

Xiao Liu, Junjian Li, Bruno Loureiro Cadilha, Anamarija Markota, Cornelia Voigt, Zhe Huang, Peter P. Lin, Daisy D. Wang, Juncheng Dai, Gisela Kranz, Anna Krandick, Darko Libl, Horst Zitzelsberger, Isabella Zagorski, Herbert Braselmann, Min Pan, Sibo Zhu, Yuanchi Huang, Sebastian Niedermeyer, Christoph A. Reichel, Bernd Uhl, Daria Briukhovetska, Javier Suárez, Sebastian Kobold, Olivier Gires*, Hongxia Wang*

*Corresponding author. Email: olivier.gires@med.uni-muenchen.de (O.G.); whx365@126.com (H.W.)

Published 19 June 2019, *Sci. Adv.* **5**, eaav4275 (2019)
DOI: 10.1126/sciadv.aav4275

This PDF file includes:

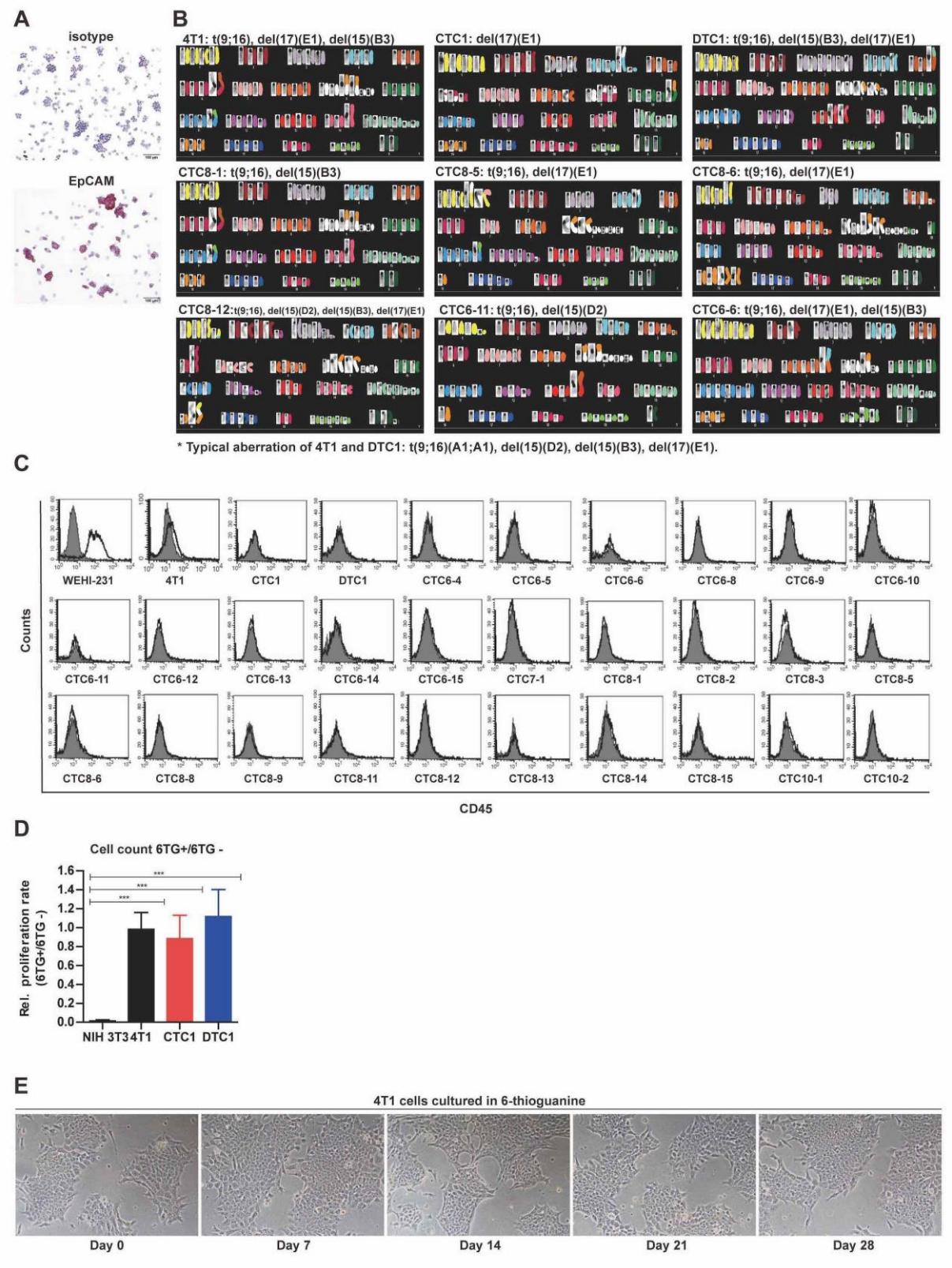

Fig. S1. EpCAM and CD45 expression, karyotyping, and 6-thioguanine effects on 4T1 cells and sublines. (**A**) Immunocytochemistry staining of EpCAM on cytospins of 4T1 cells. Shown are representative staining from n = 3 independent experiments. (**B**) Karyotype analysis of 4T1, CTC1,

DTC1, and DTC1-derived CTC sublines CTC8-1, CTC8-5, CTC8-6, CTC8-12, CTC6-11 and CTC6-6. Shown are representative karyotypes including color-coded chromosomes, chromosome numbers, and marker mutations. Typical aberrations of 4T1 and DTC1 (t(9;16)(A1;A1), del(15)(D2), del(15)(B3), del(17)(E1)) were also found in CTC sublines. del: deletion; der: derived; dmin: double minute chromosomes; mar: marker chromosome; rob: Robertsonian translocation; t: translocation. (**C**) CD45 expression on 4T1-derived sublines. Expression of leukocyte marker CD45 on the cell surface of 4T1, CTC1, DTC1 and DTC1-derived CTC sublines was measured by flow cytometry with CD45-specific antibodies(black) and isotype controls (grey). Murine B cell lymphoma cell line WEHI-231 was used as a positive control. Shown are representative histograms. (**D**) 6-TG resistance of 4T1, CTC1 and DTC1 cell lines. 4T1, CTC1, and DTC1 cell lines and murine NIH3T3 fibroblast cells were plated at equal cell numbers (initial cell number 5000 cells). Relative proliferation rates were calculated at day 5 as cell numbers in 6-thioguanine (6-TG) containing medium divided by cell numbers in medium without 6-TG. NIH 3T3 cells were used as a negative control based on their sensitivity towards 6-TG. Shown are mean ratios with SD of $n \geq 3$ independent experiments performed in duplicates. One-way ANOVA with *posthoc* multiple testing and Bonferroni correction; *** < 0.001. (**E**) 4T1 cells were cultured for the indicated 28 days in the presence of 6-TG and cell morphology was assessed at the indicated time points. Shown are representative points of treated cultures.

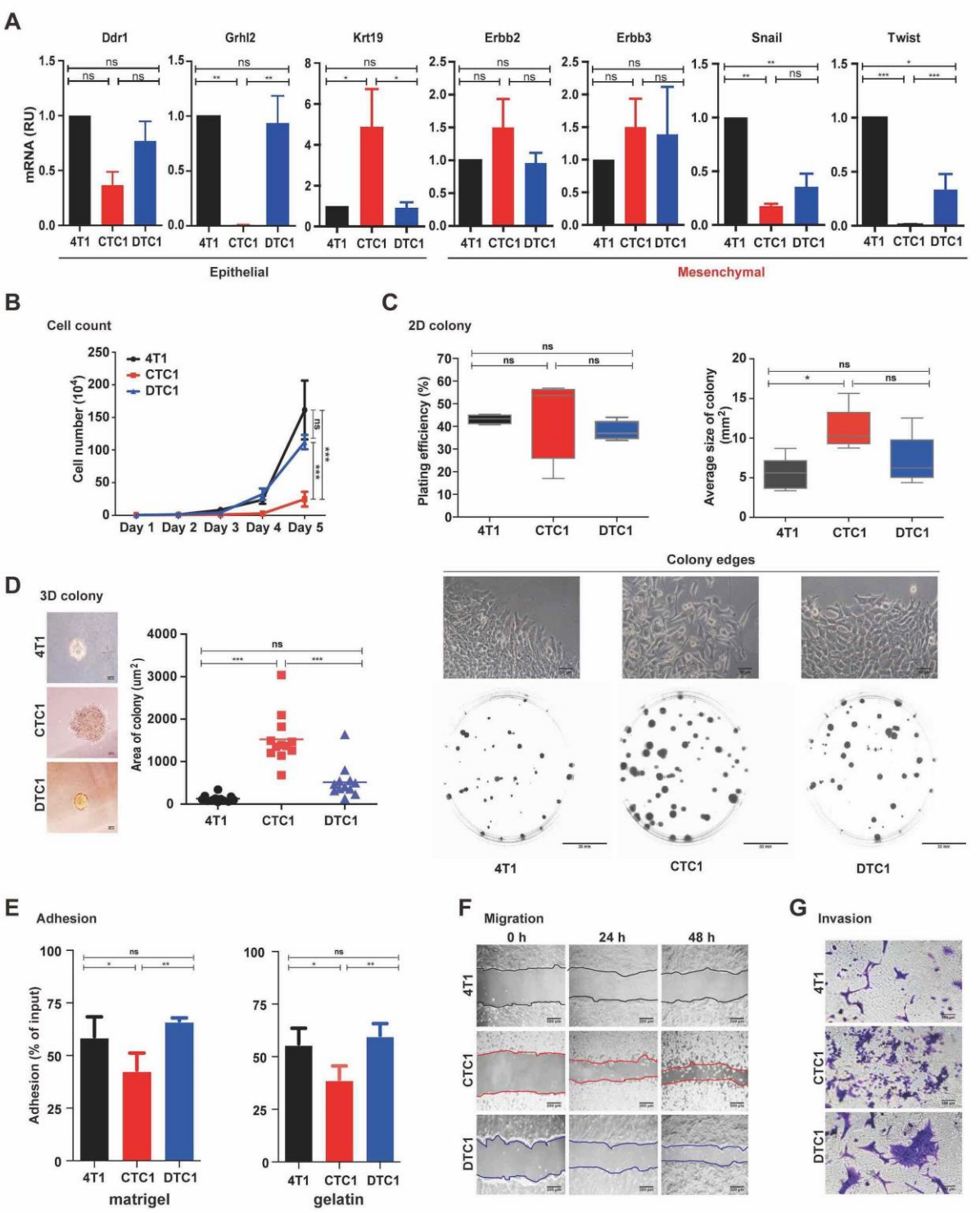

Fig. S2. Quantification of EMT markers, cell growth, 2D and 3D colony formation, cell adhesion, migration, and invasion of 4T1 cells and sublines CTC1 and DTC1. (**A**) mRNA transcript levels of epithelial markers Ddr1, Grhl2 and Krt19, and of EMT markers Erbb2, Erbb3, Snail and Twist in 4T1, CTC1 and DTC1 were assessed upon qRT–PCR with specific primers and GUSP as a house-keeping gene. Shown are mean with SD from n = 3 independent experiments

performed in triplicates. One-way ANOVA with *posthoc* multiple testing and Bonferroni correction; ns: not significant, * < 0.05, ** < 0.01, *** < 0.001. (**B**) Proliferation rate of 4T1, CTC1, DTC1 was assessed by cell counting (initial cell number 5000 cells). Shown are mean with SD from n ≥ 4 independent experiments. One-way ANOVA with *posthoc* multiple testing and Bonferroni correction; ns: not significant, *** < 0.001. (**C**) 2D colony formation assay was performed with 4T1, CTC1, and DTC1 cells. Left panel: Plating efficiency is shown as box-plot whiskers graph with mean and SD from n = 4 independent experiments performed in unicates. One-way ANOVA with *posthoc* multiple testing and Bonferroni correction; ns: not significant. Lower panels: Representative images of crystal violet-stained colonies from each cell line and 2D colony edges are shown from 4T1, CTC1, and DTC1 cells at an initial seeding density of 200 cells. Right panel: Colony sizes were calculated using Image J software and are represented as box-plot whiskers graph with mean and SD. One-way ANOVA with *posthoc* multiple testing and Bonferroni correction; ns: not significant, * < 0.05. (**D**) 3D colony formation assay was performed with 4T1, CTC1, and DTC1 cells. Representative images of colonies from 4T1, CTC1, and DTC1 cells are shown. Quantification of 3D colony size is shown (right panel) as dot plots with mean from n = 12 randomly selected colonies for each cell lines. One-way ANOVA with *posthoc* multiple testing and Bonferroni correction; ns: not significant, *** < 0.001. (**E**) Adhesion assay to matrigel and gelatin was performed with 4T1, CTC1, and DTC1 cells. Shown are mean adhesion rate with SD from n ≥ 3 independent experiments performed in triplicates. One-way ANOVA with *posthoc* multiple testing and Bonferroni correction; ns: not significant, * <0.05, ** < 0.01. (**F**) Migration capacity of 4T1, CTC1 and DTC1 was assessed in a scratch assay. Representative images of cellular migration were taken at times 0 h, 24 h and 48 h. (**G**) The invasion capacity of 4T1, CTC1, DTC1 cells was detected by transwell invasion assay. Representative images of invasive cells are shown (n = 3 independent experiments).

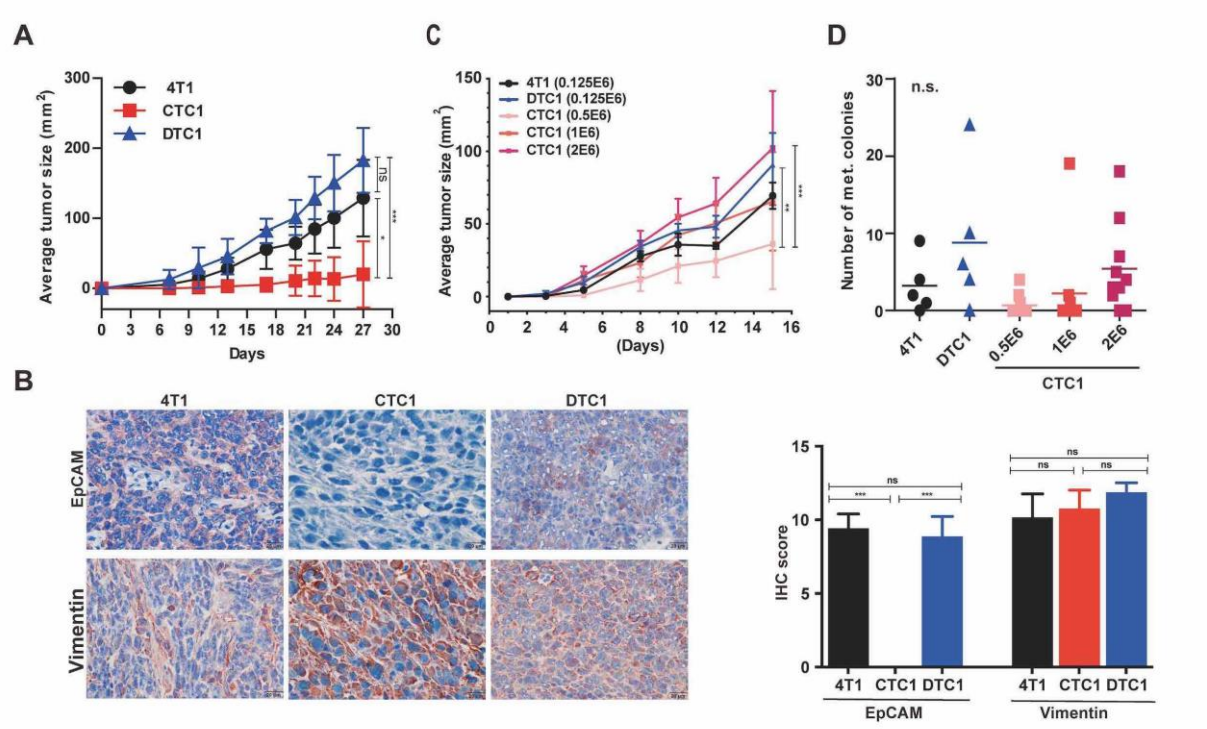

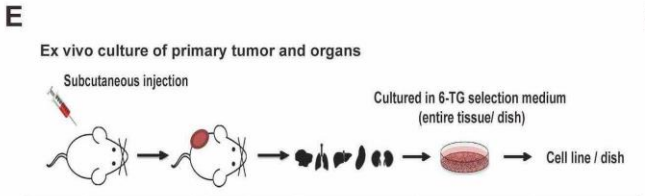

	Primary tumor		Lung		Liver		Kidney		Spleen	
	Derived cell line	Input	Derived cell line	Input	Derived cell line	Input	Derived cell line	Input	Derived cell line	Input
4T1	8	8	4	8	0	8	0	8	0	8
CTC1	4	4	3	13	0	13	0	13	1	13
DTC1	3	3	3	5	0	5	2	5	1	5

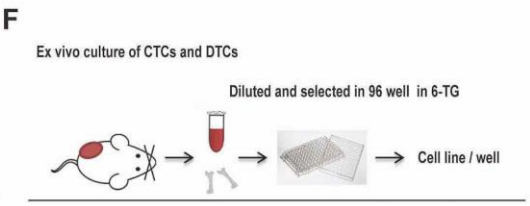

	Blood (CTC)			Bone marrow (DTC)		
	Derived cell line	Output (No. mouse)	Input (No. mouse)	Derived cell line	Output (No. mouse)	Input (No. mouse)
4T1	1 (CTC1)	1	13	1 (DTC1)	1	13
CTC1	0	0	17	0	0	13
DTC1	26	4	8	10	2	8

CTC positive incidence: $P_{(DTC1\ vs\ CTC1)} = 0.048$

G

Cells	Gene name
Both in 4T1 and DTC1	Fbxw7, Ntrk1, Prcc, Muc1, Tpm3, Bcl7a, Hnf1a, Chek2, Mn1, Ptpn11, Crlf2, Alk
Significantly exclusive in 4T1	Ep300, Pdgfb, Myh9, Cblb, Tfg
Significantly exclusive in DTC1	Ackr3, Set, Fnbp1, Abl1, Nup214, Cntrl, Hsp90aa1, Akt1, Bcl11b, Birc3, Maml2, Crebbp, Ciita, Socs1, Tnfrsf17, Ercc4, Myh11

H

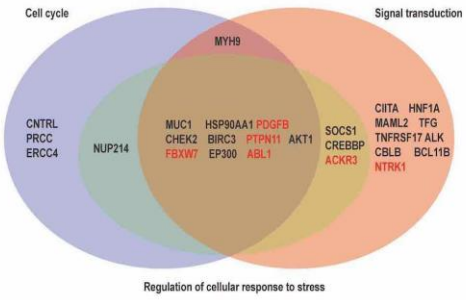

I

Term	Count	P value
Positive regulation of ERK1 and ERK2 cascade	6	0.006
Cellular response to UV	4	0.013
Regulation of mRNA stability	3	0.018
Regulation of cellular response to hea	4	0.020
Platelet formation	3	0.053
Peptidyltyrosine phosphorylation	6	0.062
G2/M transition of mitoticell cycle	3	0.076
Phosphorylation	3	0.076
Protein autophosphorylation	5	0.088

Fig. S3. Analysis of tumor growth, metastases formation, EpCAM and vimentin expression, ex vivo cultures, and GO terms and genes associated with DNA breakpoints

in 4T1 cells and sublines CTC1 and DTC1. (**A**) 4T1, CTC1, and DTC1 ($1.25*10^5$ cells) were transplanted subcutaneously into BALB/c mice. Line charts show tumor growth curves for each group as mean with SD. One-way ANOVA with *posthoc* multiple testing and Bonferroni correction; ns: not significant, * <0.05, *** < 0.001. (**B**) Shown are representative immunohistochemistry (IHC) staining of EpCAM and vimentin in primary tumors from 4T1, CTC1 and DTC1 cells injected group (left panel) and quantified IHC scores (see Materials and Methods) across all tumors. One-way ANOVA with *posthoc* multiple testing and Bonferroni correction; ns: not significant, *** < 0.001. (**C**) 4T1 and DTC1 cell number in $1.25*10^5$, whereas CTC cell numbers in $0.5*10^6$, 10^6, and $2*10^6$ were transplanted subcutaneously into BALB/c mice. Line charts show tumor growth curves for each group as mean with SD. One-way ANOVA with *posthoc* multiple testing and Bonferroni correction; ns: not significant, ** < 0.01, *** < 0.001. (**D**) Metastasis colony formation assay was performed as described in Materials and Methods. Dot plots show numbers of colonies including mean (line). No significant difference was detected between groups. (**E**) *Ex vivo* establishment of primary tumor and metastatic cell lines. Schematic representation of *ex vivo* set-up of cell lines from primary tumors and metastatic sites (lung, spleen, liver and kidney). Table shows frequencies of successfully established cell lines from input. (**F**) *Ex vivo* establishment of CTCs and DTCs. Schematic representation of *ex vivo* set-up of CTC and DTC lines from blood and bone marrow. Table shows frequencies of successfully established cell lines from input. (**G**) Cancer genes extracted from genomic regions affected by chromosomal aberrations defined as significantly different between 4T1 and DTC1 cells. Shown are genes from aberrations present in 4T1 and DTC1 with different frequencies and genes from exclusive aberrations. (**H**) Venn diagram representing 27 potentially affected breakpoint genes that are assigned to three superordinated GO-terms (cell cycle, signal transduction, regulation of response to stress). Six genes marked in red are part of the most important downstream GO-term "*Positive regulation of ERK1 and ERK2 cascade*". The remaining genes are part of other GO-terms. (**I**) GO-term enrichment analysis of 34 genes listed in (G). GO-terms were referenced to the selected cancer genes. The top 10 GO-terms are depicted.

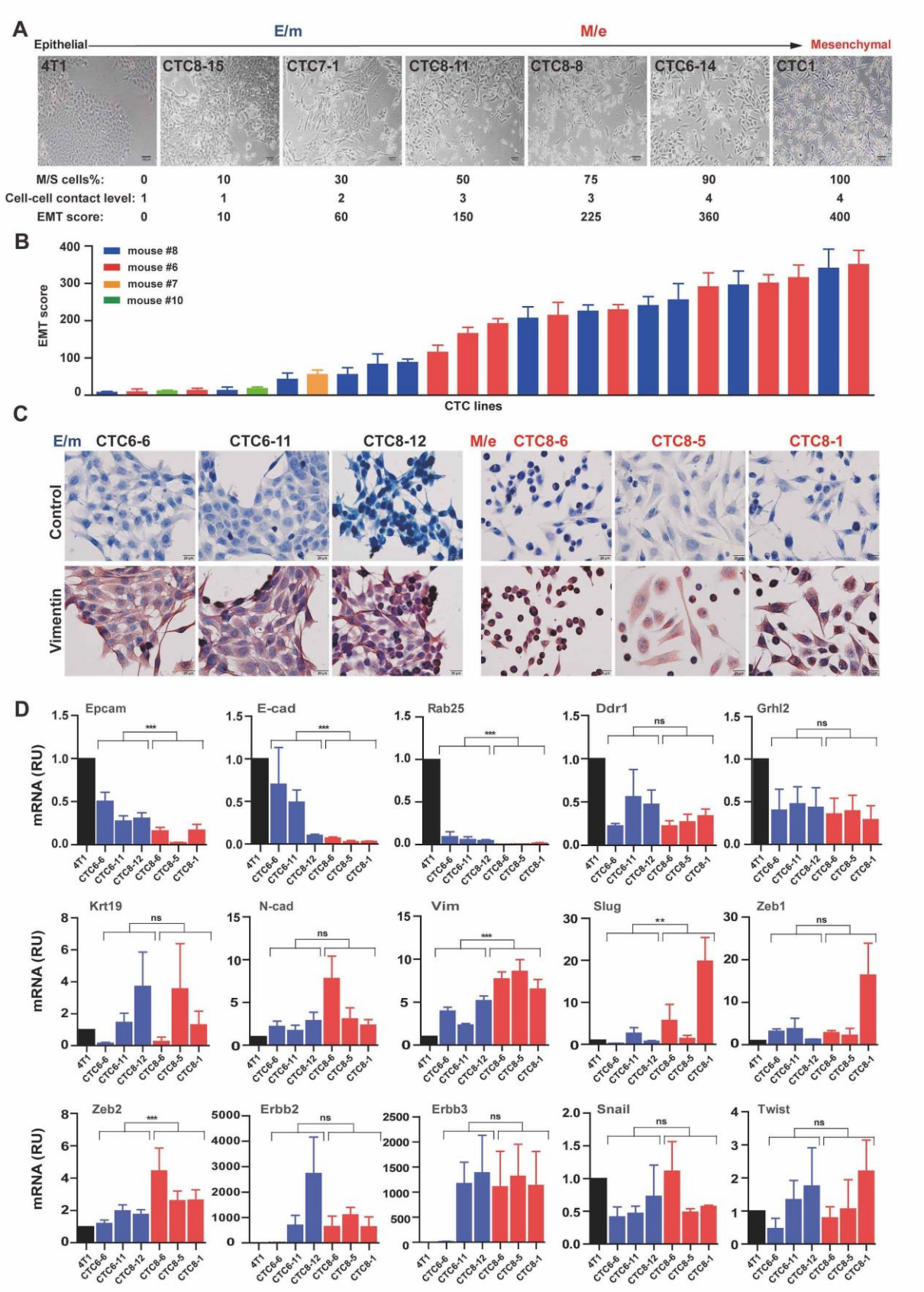

Fig. S4. Analysis of EMT scores and markers in 4T1 cells, E/m- and M/e-type sublines.

(**A**) Epithelial and mesenchymal phenotypes of 4T1, CTC1, and CTC lines generated from mice re-

transplanted with DTC1 cells were assessed. Shown are representative pictures of CTC1, 4T1 and CTCs displaying various degrees of EMT (upper panels). EMT score is presented as product of percentage of mesenchymal/spindle shape cells and cell-cell contact level (see Materials and Methods). (**B**) EMT score for 4T1, CTC1, and DTC1-derived CTC lines is presented as mean with SD from n = 4 experiments. Mice of origin are color-coded in the bar graph. (**C**) Immunohistochemistry staining of vimentin and control in E/m-type (CTC6-6, CTC6-11, CTC8-12) and M/e-type (CTC8-6, CTC8-5, CTC8-1) CTCs derived from DTC1 transplantations. Shown are representative pictures from n = 3 staining. (**D**) mRNA transcript levels of epithelial markers Epcam, E-cad, Rab25, Ddr1, Grhl2, Krt19, and mesenchymal maker N-cad, Vim, Slug, Zeb1/2, Erbb2/3, Snail, Twist in E/m-type (CTC6-6, CTC6-11, CTC8-12) and M/e-type (CTC8-6, CTC8-5, CTC8-1) CTCs derived from DTC1 transplantations, with 4T1 cells as a reference set to 1. Shown are mean with SD from n = 3 independent experiments performed in triplicates. T-test E/m versus M/e cells is indicated; ns: not significant, * <0.05, ** < 0.01, *** < 0.001.

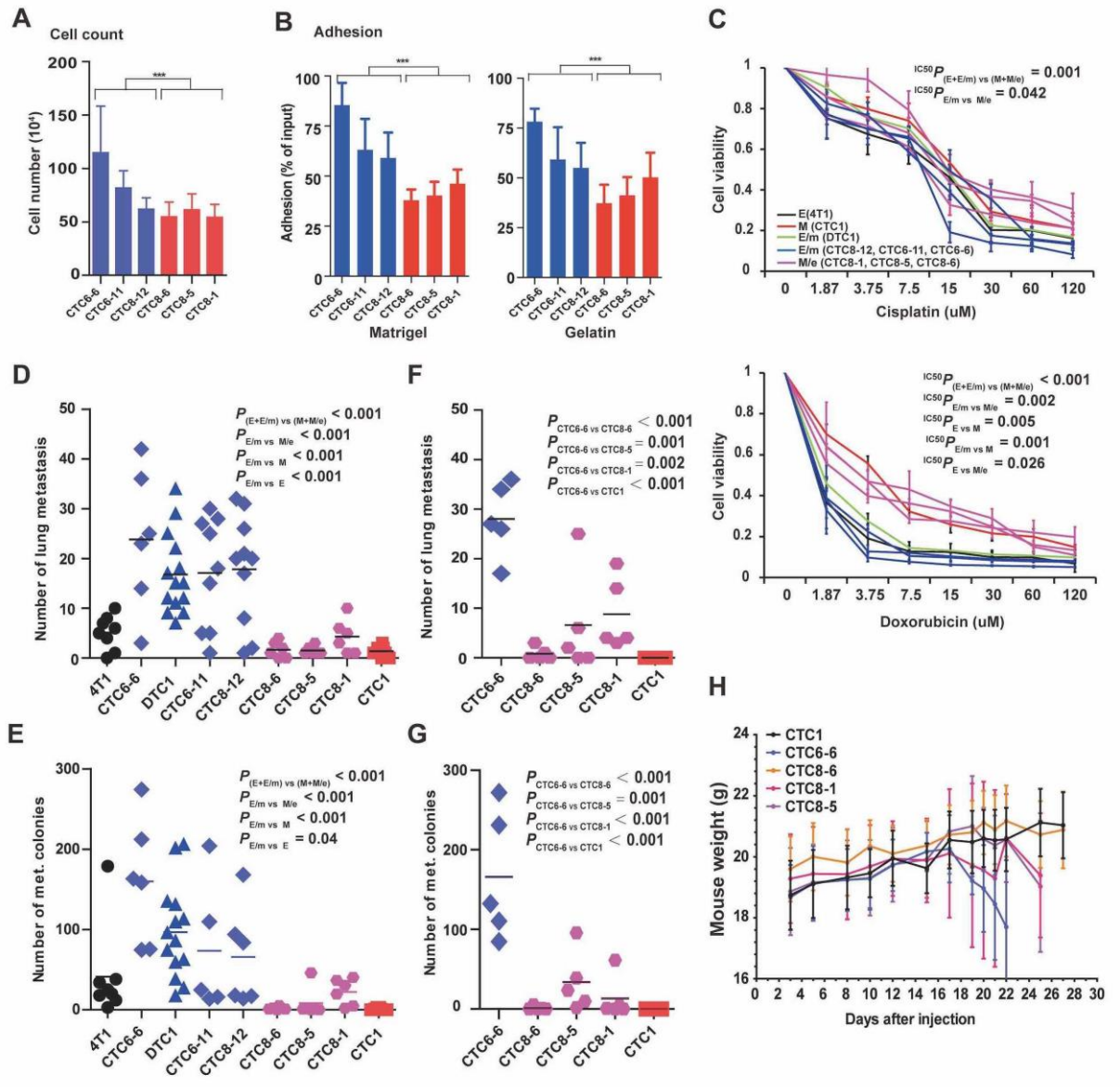

Fig. S5. Analysis of cell proliferation, adhesion, sensitivity to chemotherapy, and metastasis formation in 4T1 cells, E/m-, M/e-, and M-type sublines. (**A**) Cell proliferation of E/m-type (CTC6-6, CTC6-11, CTC8-12) and M/e-type (CTC8-6, CTC8-5, CTC8-1) CTCs derived from DTC1 transplantations (initial seeding number 5000 cells, cell numbers were counted on day 5). Shown are mean with SD from n=4 independent experiments. T-test E/m versus M/e cells is indicated; *** < 0.001. (**B**) Adhesion assay to matrigel and gelatin was performed with E/m-type (CTC6-6, CTC6-11, CTC8-12) and M/e-type (CTC8-6, CTC8-5, CTC8-1) CTCs. Shown are mean adhesion rate with SD from n ≥ 3 independent experiments performed in triplicates. T-test E/m versus M/e cells is indicated; *** < 0.001. (**C**) Chemoresistance towards cisplatin and doxorubicin was tested across a

concentration range of 1.875 - 120 µM by MTT assay in the indicated cell lines. Shown are viability curves with SD from n = 3 independent experiments performed in triplicates. Statistical analysis was done by comparing IC_{50} values. One-way ANOVA with posthoc multiple testing and Bonferroni correction*, p-values is indicated. (**D-E**) **D**: Epithelial E-type (4T1), E/m-type (CTC6-6, CTC6-11, CTC8-12, DTC1), M/e-type (CTC8-6, CTC8-5, CTC8-1) and mesenchymal M-type (CTC1) cells were transplanted into mice through tail vein injection. After 19 days, numbers of superficial lung metastasis were counted and lungs were harvested for further metastasis colony formation assay. Dot plots show numbers of metastasis counted in lungs including mean (line) and p-values. **E**: Metastasis colony formation assay was performed (Materials and Methods) and is displayed as dot plots showing numbers of colonies including mean (line). One-way ANOVA with *posthoc* multiple testing and Bonferroni correction*, p-values is indicated. (**F-G**) E/m-type (CTC6-6), M/e-type (CTC8-6, CTC8-5, CTC8-1) and mesenchymal M-type (CTC1) cells were transplanted into mice through tail vein injection. Each experimental group was ended at indicated signs of endpoint. **F:** Dot plots show numbers of metastasis counted in lungs including mean (line) and p-values. **G**: Metastasis colony formation assay was performed and is displayed as dot plots showing numbers of colonies including mean (line). One-way ANOVA with *posthoc* multiple testing and Bonferroni correction*, p-values is indicated. (**H**) Line charts shows mouse weight curves for each group as mean with SD.

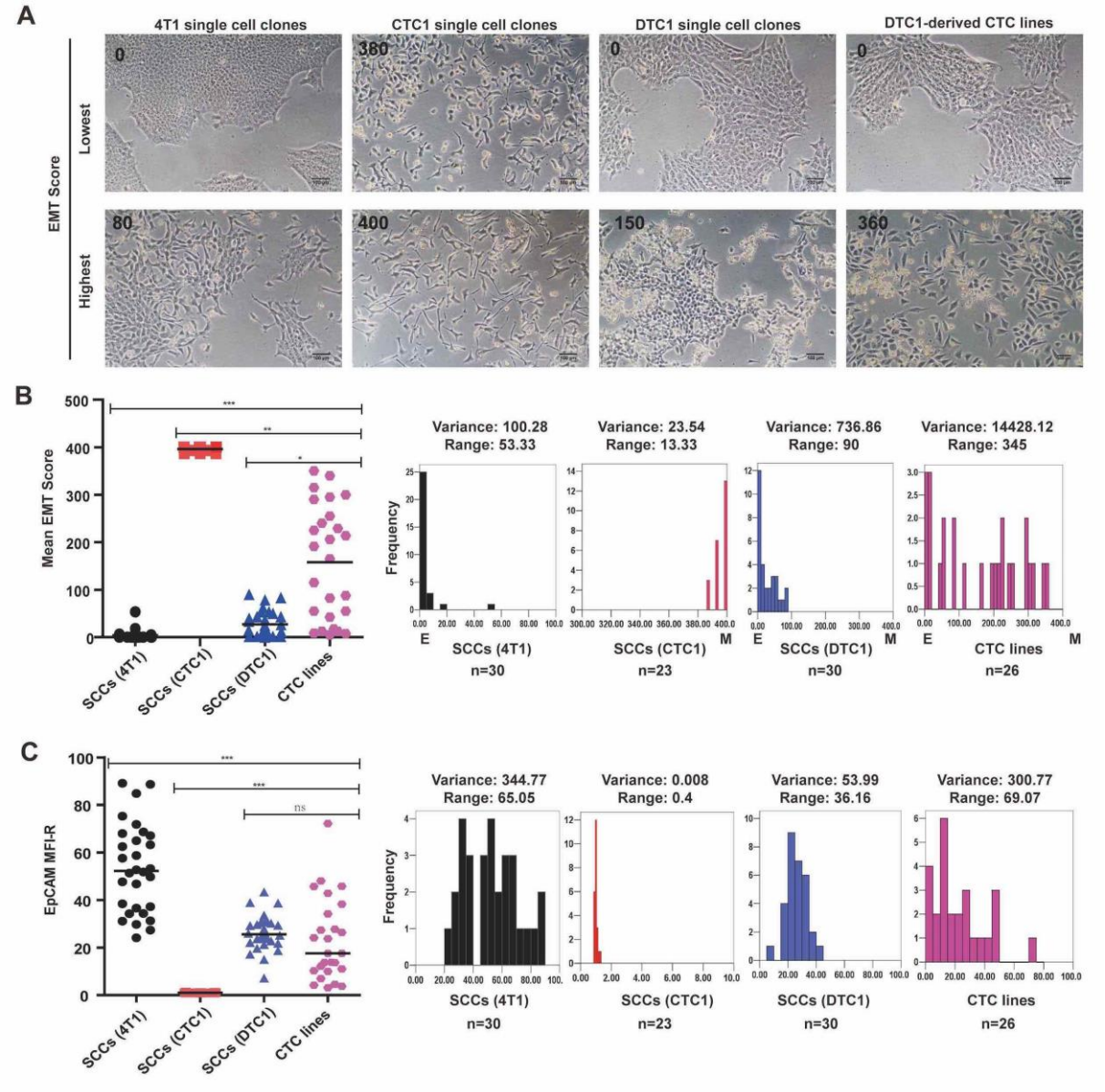

Fig. S6. Analysis of morphology, EMT scores, and EpCAM expression of 4T1-, CTC1-, and DTC1-derived single cell clones, and DTC1-derived CTC sublines. (**A**) Single cell clones were generated from 4T1 (n = 30), CTC1 (n = 23), and DTC1 cells (n = 30). Shown are representative pictures of 4T1, CTC1, DTC1 single cell clones and DTC1-derived CTC lines (n = 26) with highest and lowest EMT scores. (**B**) Dot plots shows mean values of EMT scores in 4T1, CTC1, DTC1 single cell clones and DTC1-derived CTC lines from n = 3 independent scoring. The degree of EMT score dispersion in each group is shown as frequency diagrams with variance (squared value of standard deviation) and range (difference between lowest and highest values). Kruskal-wallis test with *posthoc* multiple testing and Dunn´s correction, * < 0.05, ** < 0.01, *** < 0.001. (**C**) Dot plots shows

means of EpCAM expression in 4T1, CTC1, DTC1 single cell clones and DTC1-derived CTC lines from n = 2 initial measurements. The degree of EpCAM expression dispersion in each group is shown as frequency diagrams with variance and range. One-way ANOVA with *posthoc* multiple testing and Bonferroni correction, *** < 0.001.

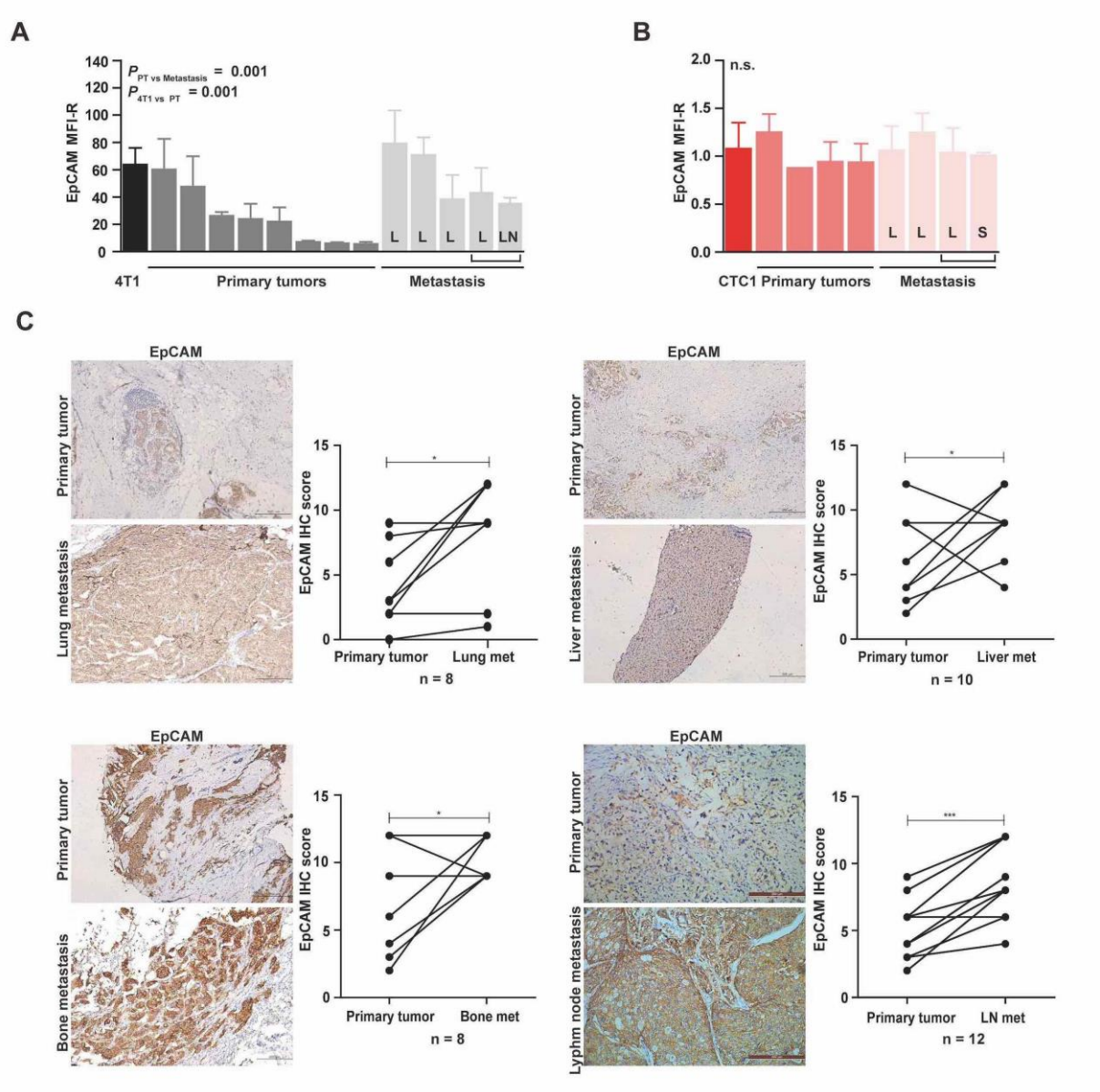

Fig. S7. EpCAM expression in 4T1- and CTC1-derived primary tumors and metastases, and in primary tumors, lymph node and distant metastases of clinical samples of MBC.

(**A-B**) EpCAM expression in 4T1 derivative cell lines. EpCAM expression was measured by flow cytometry in permanent cell lines originating from primary tumor and metastases generated following re-transplanted of 4T1 (left panel) and CTC1 cells (right panel) into BALB/c mice. Brackets demark cell lines originating from one individual mouse. L: lung, S: spleen, LN: lymph node. Data is presented as mean fluorescence intensity ratios (EpCAM/control) with SD. Shown are mean MFI-R with SD from n ≥ 3 independent experiments performed in unicates. One-way ANOVA with posthoc multiple testing and Bonferroni correction*; p-values is indicated ns: not significant. (**C**) EpCAM

expression level was assessed in n = 38 human breast tumors. Shown are representative immunohistochemistry (IHC) staining of EpCAM in primary tumors and corresponding metastatic sites (lung, liver, bone marrow, lymph node) and the quantification of EpCAM IHC scores of paired tumor and metastases samples (see Materials and Methods). Paired T test; * < 0.05, *** < 0.001.

A

Characteristic	No. (%)
Total no. of patients	34 (100)
Gender	
Female	34 (100)
Age (years)	
Median	57
Range	28-76
Tumor stage	
Stage IIIa	1 (2.94)
Stage IIIc	10 (29.41)
Stage IV	23 (67.65)
Intrinsic Subtype	
Luminal A	6 (17.65)
Luminal B	15 (44.12)
HER2 +	9 (26.47)
HER2 -	6 (17.65)
HER2 positive (non-luminal)	7 (20.59)
Triple negative (basal-like)	4 (11.76)
Normal-like	2 (5.88)
Follow-up (Months)	
Median	11
Range	1-28
Distant detectable metastases	
Lung	5 (14.71)
Bone	5 (14.71)
Liver	4 (11.76)
Others	2 (5.88)
Multiple	7 (20.59)
Numbers of detected CTC per patient	
Median	9
Range	1-185
Numbers of detected DTC per patient	
Median	413
Range	4-40240

HER2 = human epidermal growth factor receptor 2.

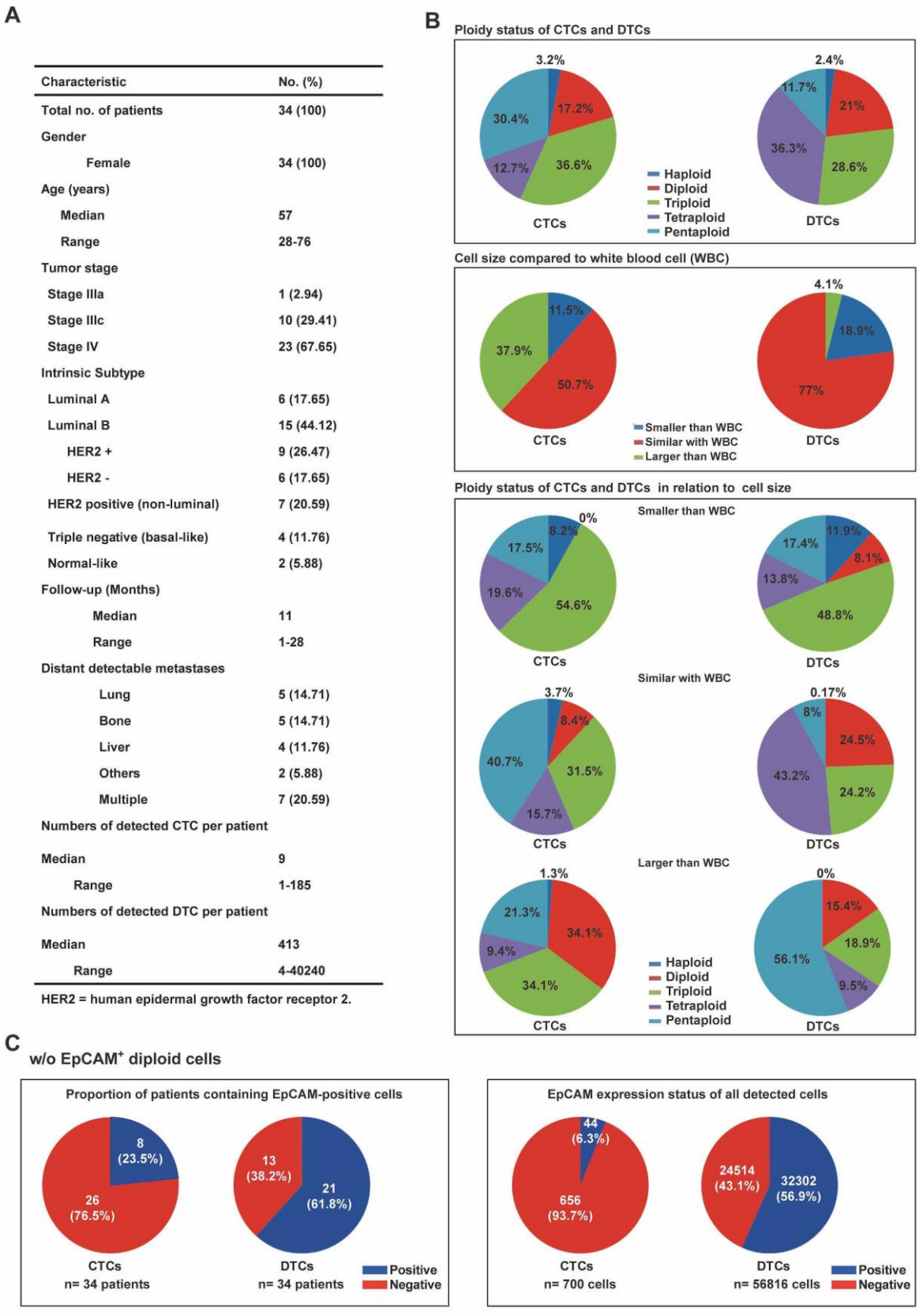

Fig. S8. Patients' characteristics and ploidy and cell size of CTCs and DTCs from MBC patients. (**A**) Patients' characteristics. Shown are clinical parameters for n=34 MBC patients

including gender, age, tumor stage, subtype, follow-up time in months, distant metastases, CTC and DTC numbers. (**B**) Characterization of chromosome 8 ploidy and cell size compared to white blood cells (WBC) in CTCs and DTCs isolated from breast cancer patients. Shown are frequencies of differential ploidy statuses and cell size compared to WBC in percent for CTC and DTC from n=34 MBC patients. Additionally, the ploidy status is depicted in relation to CTC and DTC size compared to WBC (lower panels). (**C**) Shown are proportions of $EpCAM^+$ CTC and DTC in individual patients (n = 34) (left pie charts) and in overall numbers of CTC (n = 700) and DTC cells (n = 56,816) (right pie charts). Blue: $EpCAM^+$, red: $EpCAM^-$. Data exclude $EpCAM^+$ diploid CTC and DTC, and represent exclusively aneuploid cells.

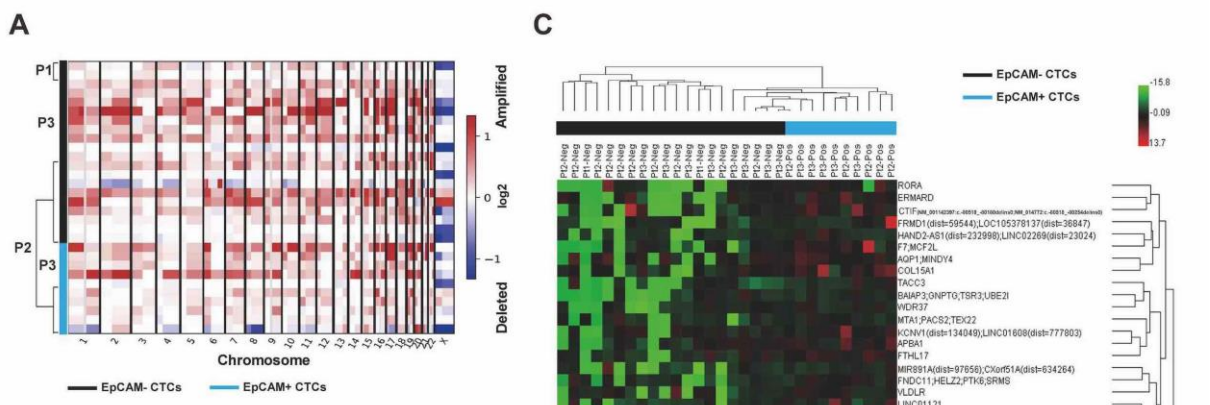

B

Chromosome	NO. of CNVRs	No. of genes	Total length of CNVRs (bp)
1	65	128	3249107
2	64	94	3199142
3	44	82	2200491
4	29	46	1450565
5	45	78	2250786
6	32	52	1597679
7	28	52	1400012
8	24	54	1202875
9	33	55	1656598
10	27	42	1350461
11	29	65	1450727
12	36	61	1800333
13	18	22	900461
14	13	22	649922
15	27	61	1351108
16	25	59	1249948
17	31	108	1549902
18	10	14	499777
19	20	77	999275
20	16	25	799888
21	9	18	449844
22	10	33	500390
X	16	15	800046
Y	6	8	299910
Total	657	1255 (Duplication removed)	32859247

Fig. S9. Copy number variations in EpCAM$^+$ and EpCAM$^-$ CTCs from MBC patients.

Shown are CNV on all chromosomes with numbers of CNV regions, genes, and length of CNV regions. Unsupervised clustering of top 100 CNV in in EpCAM$^+$ and EpCAM$^-$ CTC. (A) Visualization of copy number variation (CNV) profiles in n=10 EpCAM$^+$ (light blue) and n=20 EpCAM$^-$ single CTCs (black). Within the chromosome plots, red indicates DNA copy number amplifications and blue indicates deletions in log2 scale. (B) Chromosome distribution of significantly different CNV regions

(CNVRs) between EpCAM^{+} and EpCAM^{-} CTCs. Listed are chromosomes, numbers of CNVRs, numbers of genes affected and total length of CNV regions in base pairs (bp). (C) Shown is an unsupervised clustering of the top 100 CNV, including genes encoded in the genomic regions affected by the CNV between EpCAM^{+} (light blue) and EpCAM^{-} CTCs (black). CTCs originated from n = 3 patients, which are denoted as Pt1-3.

Table S1. Enrichment analysis of GO biological process terms of CNVs from EpCAM^{+} and EpCAM^{-} CTCs. Enrichment analysis of GO biological process terms was carried out with in 657 CNVs comprising 1255 genes obtained from EpCAM^{+} vs EpCAM^{-} CTCs. Shown are all terms with p-value < 0.05. Genes marked in red font were amplified, genes marked in green font were deleted.

Term	Gene count	%	P Value	Enrichment Score	Genes
Peptidyl-tyrosine dephosphorylation	12	1.447527	0.000346	3.460445	MTM1, PTPN6, DUSP3, PTPRD, CDC14A, PTPN3, UBASH3B, PTPRN2, PTPN13, PTPRT, PTPRQ
Endoplasmic reticulum organization	6	0.723764	0.001541	2.812319	TOR1AIP2, DNM1L, BNIP1, VAPB, ATL1, EIF2AK3
Negative regulation of canonical Wnt signaling pathway	14	1.688782	0.002451	2.610573	CSNK1A1, NKD2, BICC1, PARK2, WWTR1, TMEM64, GLI1, SFRP5, RGS20, GPC3, SOST, PSMB6, SCYL2, PSMD1
Microtubule-based movement	9	1.085645	0.004561	2.340949	KIF22, CLTA, KIF1A, DNAH14, DNAH17, KIF9, SH3GL2, DYNC1I2, DNAH6
Nervous system development	19	2.291918	0.005729	2.241948	ERBB4, MAFB, NLGN1, DPYSL5, DPYSL2, ARID1B, SLC7A5, SMN1, ARHGAP26, P2RX5, MEF2D, MYT1L, NAV2, MTR, CNTN4, NAIP, DLG2, ZNF423, DLG1
Mammary gland epithelial cell differentiation	4	0.482509	0.00751	2.124341	AKT1, PRLR, ERBB4, MGMT
Protein dephosphorylation	11	1.3269	0.007694	2.113842	MTM1, PTPN6, PTPRD, PTPN3, CPPED1, PTPRN2, PPP3R1, PTPN13, PTPRT, LHPP, DLG1
Phospholipid biosynthetic process	6	0.723764	0.008908	2.050225	PGS1, LPCAT1, PEMT, PCYT1A, AGPAT3, LPCAT3
Neural retina development	4	0.482509	0.009332	2.030015	RAB11FIP4, SLC17A8, ACTL6A, TGFB2
Microspike assembly	3	0.361882	0.009747	2.011145	MTSS1, ACTN2, ABL1
Mammary gland duct morphogenesis	3	0.361882	0.009747	2.011145	GLI2, SCRIB, CSF1R
Neuronal action potential	5	0.603136	0.011882	1.925105	P2RX4, CATSPER4, SCN1A, CHRNA1, GPR88
Positive regulation of mitotic cell cycle	5	0.603136	0.011882	1.925105	CCNB1, SHB, EIF4EBP1, DUSP3, ABL1
Insulin secretion involved in cellular response to glucose stimulus	3	0.361882	0.014309	1.844389	RAB11FIP5, PTPRN2, RAB11B
Positive regulation of establishment of protein localization to plasma membrane	5	0.603136	0.015121	1.820428	AKT1, EZR, NKD2, DPP10, DLG1
Mammary gland alveolus development	4	0.482509	0.016228	1.789727	PRLR, ERBB4, PHB2, ESR1
Transport	20	2.412545	0.018401	1.735169	CREBRF, SLC20A2, GRIK4, SLC12A5, UNC50, CACNG2, SLC7A5, SEC14L1, ABCG2, P2RX5, RAB11FIP4, P2RX4, SEC22A, SLC13A2, PITPNC1, CLVS1, SLC25A39, SLC51A, CHRNA1, SLC27A4
Bicellular tight junction assembly	5	0.603136	0.018866	1.724313	CLDN3, MPP5, STRN, PTPN13, DLG1
Peptidyl-serine phosphorylation	10	1.206273	0.020018	1.698588	CSNK1A1, AKT1, STK32A, CSNK1G1, TTBK2, MORC3, LMTK2, PRKCH, EIF2AK3, DMPK
Regulation of mitophagy	5	0.603136	0.020936	1.679113	DNM1L, ATG7, BNIP3L, ACTL6A, SREBF2
Cell differentiation	24	2.895054	0.027298	1.563874	SRPK2, PTPN6, RMDN3, APOLD1, PRKCH, CDHR5, EDAR, NHS, SLC7A5, FOXN3, PURB, PTPRQ, SFRP5, AKT1, SHB, MYT1L, RGS20, RNF151, YIPF3, CAND1, JAK2, ETV6, ZNF423, ANGPTL4
Toxin transport	5	0.603136	0.027954	1.55356	DNAJC17, TCP1, TRIP4, RAB28, ATP6V0A1
Apoptotic process	28	3.377563	0.028827	1.540204	ZFAND6, DCC, SEPT4, GULP1, SAV1, HINT2, RASSF7, CTNNBL1, PRUNE2, SHB, DOCK1, CDCA7, CSE1L, CASP9, API5, PTPN6, RMDN3, EDAR, NOA1, NLRP1, SFRP5, MEF2D, BNIP1, BNIP2, JAK2, NAIP, GADD45A, PUF60
Positive regulation of chemokine secretion	3	0.361882	0.032209	1.492029	IL4R, C5, CSF1R
Receptor localization to synapse	3	0.361882	0.032209	1.492029	NLGN1, DLG2, DLG1
Response to endoplasmic reticulum stress	7	0.844391	0.034011	1.468384	TTC23L, CREBRF, ALOX15, PDIA5, PARK2, ABL1, EIF2AK3
Regulation of membrane potential	7	0.844391	0.034011	1.468384	KCNMA1, ASIC2, ACTN2, PXK, FAM19A4, CHRNA1, DLG1
Rransmembrane receptor protein tyrosine kinase signaling pathway	8	0.965018	0.035665	1.447763	NTRK3, CNKSR1, MTSS1, ERBB4, PTPRT, SHC3, CSF1R, BLNK
Regulation of cell shape	10	1.206273	0.037814	1.422344	CSNK1A1, EZR, CSNK1G1, TTBK2, DIAPH1, C15ORF62, BAMBI, ARAP1, CSF1R, DLG1
Cellular response to DNA damage stimulus	13	1.568154	0.037815	1.422335	VAV3, KIAA0101, MCM10, CHCHD6, RAD50, RAD51, SETX, AKT1, RAD1, CUL4A, CASP9, IRF7, ABL1
Brain development	12	1.447527	0.044552	1.351133	SEPT4, CD9, SCT, SLC17A8, VCY1B, MDGA1, CNTNAP2, CNTN4, DPYSL2, MBD3, CTNS, SLC7A11
Signal peptide processing	4	0.482509	0.045428	1.342675	SEC11A, PROZ, SPPL2A, SPCS2
Regulation of release of sequestered calcium ion into cytosol	3	0.361882	0.047162	1.326405	PTPN6, UBASH3B, DIAPH1
Signal transduction in response to DNA damage	3	0.361882	0.047162	1.326405	CASP9, ABL1, GADD45A
Positive regulation of nitric oxide biosynthetic process	5	0.603136	0.049196	1.308071	AKT1, P2RX4, ESR1, JAK2, TLR5